



HAL
open science

Modulating Electron Transfer in an Organic Reaction via Chemical Group Modification of the Photocatalyst

Ran Liu, Li Yang, Tongtong Yang, Yan Huang, Mario Barbatti, Jun Jiang, Guozhen Zhang

► **To cite this version:**

Ran Liu, Li Yang, Tongtong Yang, Yan Huang, Mario Barbatti, et al.. Modulating Electron Transfer in an Organic Reaction via Chemical Group Modification of the Photocatalyst. *Journal of Physical Chemistry Letters*, 2019, pp.5634-5639. 10.1021/acs.jpcllett.9b01970 . hal-02288619

HAL Id: hal-02288619

<https://amu.hal.science/hal-02288619>

Submitted on 15 Sep 2019

HAL is a multi-disciplinary open access archive for the deposit and dissemination of scientific research documents, whether they are published or not. The documents may come from teaching and research institutions in France or abroad, or from public or private research centers.

L'archive ouverte pluridisciplinaire **HAL**, est destinée au dépôt et à la diffusion de documents scientifiques de niveau recherche, publiés ou non, émanant des établissements d'enseignement et de recherche français ou étrangers, des laboratoires publics ou privés.

Modulating Electron Transfer in an Organic Reaction via Chemical Group Modification of the Photocatalyst

Ran Liu^a, Li Yang^b, Tongtong Yang^a, Yan Huang^a, Mario Barbatti^{*,c}, Jun Jiang^a, and Guozhen Zhang^{*,a}

^a*Hefei National Laboratory for Physical Sciences at the Microscale, School of Chemistry and Materials Science, University of Science and Technology of China, Hefei, Anhui 230026, P. R. China*

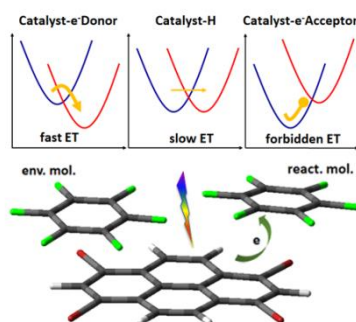
^b*Institutes of Physical Science and Information Technology, Anhui University, Hefei, Anhui 230601, P. R. China*

^c*Aix Marseille Univ, CNRS, ICR, Marseille, France.*

Abstract

Tuning electron transfer (ET) rates from catalysts to substrates is important for modulating photocatalytic organic reactions. In this work, we have taken pyrene-based photocatalysts (Py) for photocatalytic hydrodefluorination of polyfluoroarenes (FA) as model systems, and conducted a first-principle study on modulating ET rates from Py to FA via chemical modification of Py with different electron donating/withdrawing groups (EDGs/EWGs). The computed spatial distributions of frontier Kohn-Sham orbitals suggest that ET is energetically more favorable for Py-EDGs than for Py-EWGs. The estimated ET rates by a simplified Marcus model show that they are appreciably enhanced by EDGs substitution and weakened by EWGs substitution. Noticeably, the associated Gibbs free energy change plays a dominant role. Our findings of tuning ET rates for Py-FA complexes via chemical group modifications cast new insight into the rational design of metal-free photocatalysts for organic transformations.

TOC Graphic



Light-driven organic transformations have been a vibrant area in photocatalysis towards quite a few challenging synthetic goals.¹⁻⁵ Generally, they involve energy and matter conversion accompanied by a series of electron processes, including photo-induced electronic excitation, excitation energy transfer, and electron transfer (ET).⁶⁻⁷ Noticeably, in photocatalytic organic reactions, ET from photocatalysts to substrates is a central step, which activates reactants and generates reactive species.⁸ Therefore, the mechanistic understanding of the ET and subsequent modulation of ET rates have drawn intensive attention in recent years.⁹⁻¹⁵ In present work we will demonstrate how different types of functionalization of a promising class of metal-free organic chromophores can control the ET process.

Metal-free photosensitizers and photocatalysts are promising alternatives to conventional ones for photocatalytic organic synthesis, which usually comprise inorganic semiconductors¹⁶ or organometallic compounds¹⁷, because they may be inexpensive for scaling-up production, easily tunable in light adsorption, structurally flexible, and most importantly, environmentally friendly. These features have made metal-free organic chromophores appealing in recent years, drawing increasing attention in an active research field.^{4, 7} For example, Miyake and co-workers successfully developed a couple of tunable organic photosensitizer based on the dihydrophenazine and phenoxazine.¹⁸⁻²⁰ Further, *Lu et al.* performed the challenging hydrodefluorination of polyfluoroarenes (FA) using pyrene-based photocatalysts (Py), which are not only purely organic but also plays the dual role of photosensitizer and catalyst in a single compound.¹⁴ Importantly, they proposed that the “ π -hole— π ” interaction between Py and FA plays a crucial role in overcoming otherwise unfavorable energetic ET reaction that activates the C-F bond of FA. Despite of these successful examples, metal-free organic photosensitizers and photocatalysts are still scarce and not well understood yet. Therefore, it is urgent to conduct comprehensive study of the basic physical chemistry of such compounds, as we have delivered in our work. Specifically, *Lu et al.*'s discovery motivated us to conduct a theoretical study towards a comprehensive understanding of the mechanism of ET from Py to FA and the subsequent modulation of ET through molecular design.

ET reactions have been subjected to many theoretical studies.²¹ Here we are interested in a qualitative description of the tuning effect on the ET rate due to the addition of different

chemical groups to the catalyst, which can be gauged through Marcus theory.²² Nevertheless, in the framework of conventional density functional theory (DFT), the tendency of delocalization of the electron density makes it difficult to clearly define the initial and final electronic diabatic states for an ET reaction. To address this type of challenge, Van Voorhis and co-workers developed constrained density functional theory (CDFT),²³ which enables building approximate diabatic states to model the initial and final states of ET and calculate the ET rate. Therefore, we used the CDFT method in conjunction with a simplified Marcus model to describe the thermodynamics and kinetics of the ET reaction of non-bonded Py-FA complexes.

Chemical modifications with different functional groups have been a common strategy for tuning electronic properties of a molecular catalyst. Herein we selected a couple of representative electron donating groups (EDGs: $-\text{OH}$ and $-\text{NH}_2$) and electron withdrawing groups (EWGs: $-\text{CN}$, $-\text{NO}_2$, $-\text{CHO}$), all of which possess smaller steric hindrance compared to $-\text{C}\equiv\text{C}-\text{C}(\text{CH}_3)_3$ used in the previous experimental study.¹⁴ To have a more comprehensive understanding of the impact of functional groups on ET rates of Py-FA complexes, we also studied Py with substitution of $-\text{C}\equiv\text{C}-\text{C}(\text{CH}_3)_3$, $-\text{C}\equiv\text{C}-\text{CH}_3$, and $-\text{CH}=\text{CH}_2$. The schematic model of Py derivatives with various substitutions (X) is depicted in Figure 1.

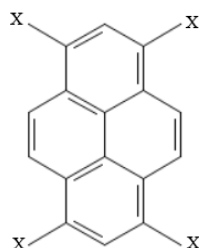
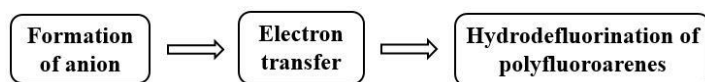


Figure 1. The model structure of the photocatalyst molecules, Py(X). (X = ($-\text{H}$, $-\text{OH}$, $-\text{NH}_2$; $-\text{CH}=\text{CH}_2$, $-\text{C}\equiv\text{C}-\text{CH}_3$, $-\text{C}\equiv\text{C}-\text{C}(\text{CH}_3)_3$; $-\text{NO}_2$, $-\text{CN}$, $-\text{CHO}$.)

We built a simplified model system consisting of one Py and two FA, i.e., Py-(FA)₂, which resembles the crystal structure reported in the *Lu et al.*'s work. To model the ET using CDFT framework, we specifically assign one of FA molecules as the electron acceptor and the other serves as an environmental factor that keeps the activated FA from moving (Figure S1).

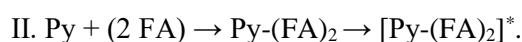
According to *Lu et al.*'s report, the whole process of the photoinduced hydrodefluorination of FA catalyzed by Py can be expressed as in the chart flow in Scheme 1, which is divided into three stages: (1) formation of the reactive anion [Py-(FA)₂]⁻; (2) electron transfer from Py to FA; (3) the hydrodefluorination of FA. In the present work, we have mainly investigated step 2, with the focus on how the substitution of different chemical groups will affect the electron transfer between Py and FA in the anionic complex.



Scheme 1. The chart flow of the photoinduced hydrodefluorination of FA catalyzed by Py

We first studied the light absorption of Py(X) and Py(X)-FA₂, and the formation and electron affinities of [Py(X)-FA₂]⁻ anions. Then, we studied the spatial distribution of frontier Kohn-Sham orbitals (FMOs) of these anions. Finally, we computed Gibbs free energy change (ΔG^0), reorganization energy (λ), and electron coupling (V_{if}) using the CDFT method, which were used to estimate the corresponding ET rate. We have found that the substitution of selected EDGs appreciably strengthens the ET from Py to FA, while the substitution of EWGs (including alkynyl and alkenyl groups) remarkably restrains the ET. In both cases, the underlying reason for the rate variation is linked with the relative values of the free energy change.

Effective light absorption by Py(X) is the prerequisite for the photocatalytic HDF of FA. We found that both EDGs and EWGs can cause a measurable red shift of the maximum absorption of Py(X) towards the visible light region and enhanced absorbance, compared to unmodified Py (Table S1). Particularly, Py with alkynyl groups exhibits an appreciable visible light absorption around 395 nm, in good agreement with experimental data in *Lu et al.*'s work. They suggest two parallel routes of the formation of excited Py-FA complexes:



All Py-(FA)₂ complexes of interest are found to have a negative binding energy ranging from -0.61 to -0.88 eV at the ωB97XD/6-311+G(d,p) level, suggesting that they are non-covalent van der Waal's (vdW) complexes and the interaction is not significantly affected by the identity of the added group (Table S3). Further, the light absorption of each Py species is almost unchanged as it forms Py-(FA)₂, indicating that the substrate has little impact on the light absorption of the photocatalyst (Table S1 and Table S2). Therefore, both pathways are equivalent for preparing the complex, which is ready for subsequent ionization.

As *Lu et al.* proposed, the excited Py-FA complex is then reductively quenched by a sacrificial electron donor and becomes an anion.¹⁴ All excited Py-(FA)₂ complexes undergo a substantial exothermic relaxation as they receive an electron (Table S4). Specifically, EWGs increases the electron affinity of the excited complex, while EDGs reduces it, compared to unmodified Py. This result suggests that EWGs tend to stabilize the excess electron attached to the complex, while EDGs have the opposite effect. Further, we compared the energy change for losing the excess electron on these relaxed Py(X)⁻ anions. Since the ET can be viewed as transition from the state of [Py]⁻-(FA)₂ to the state of Py-[FA]⁻[FA], we calculated the energy (ΔE_1) needed to detach the excess electron from the anions, to compare the tendency of ET of different Py(X): $\Delta E_1 = E[\text{catalyst}] - E[\text{catalyst}]^-$. The values of ΔE_1 in Figure 2 are indicative of the electronegativity of Py(X), which is appreciably strengthened as EWGs are added and weakened as EDGs are added. This distinction causes a drastic change in the subsequent ET reaction, as we shall see.

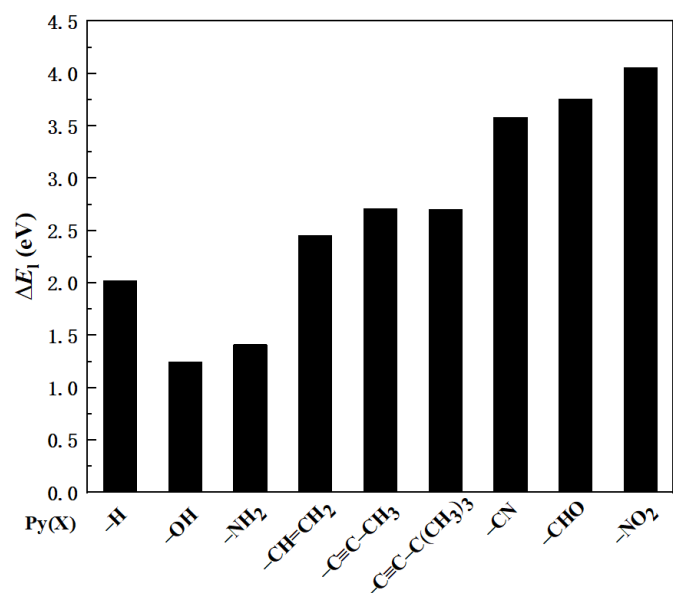


Figure 2. The energy needed for removing an electron from various $[\text{Py}(\text{X})]^-$ anions.

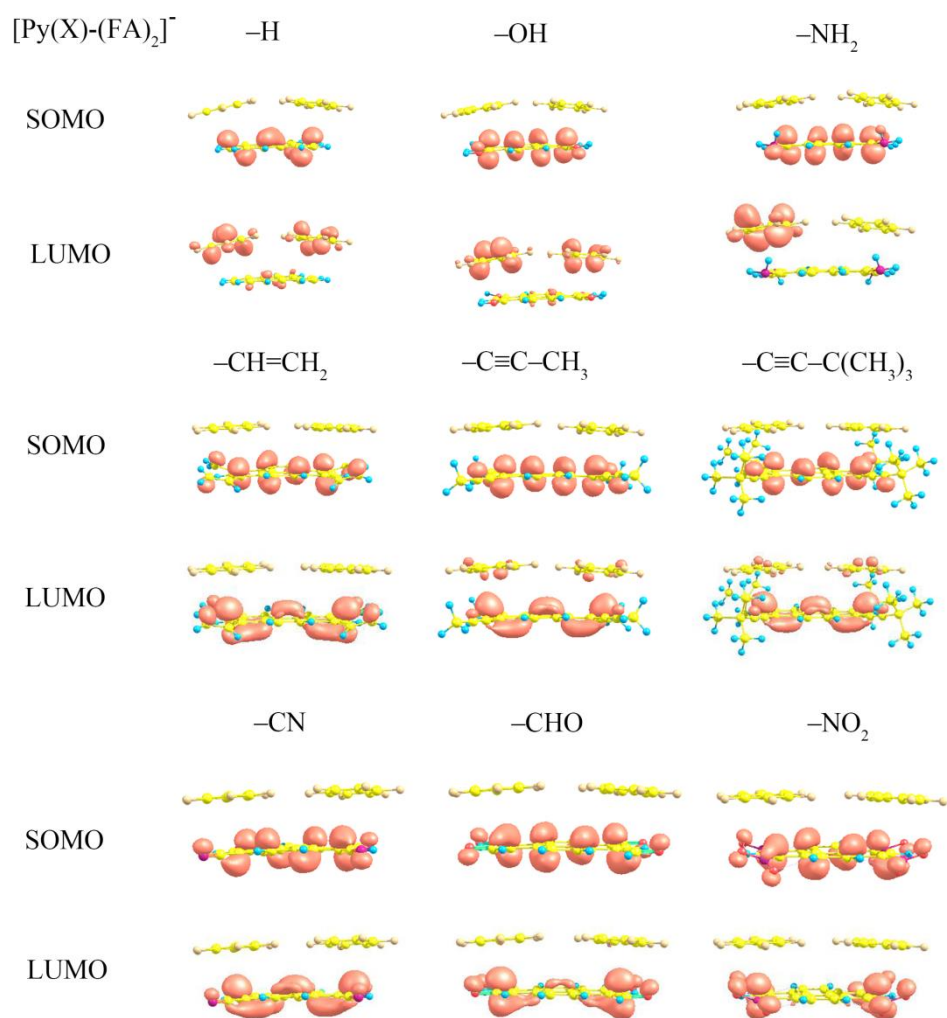


Figure 3. The spatial distribution of frontier Kohn-Sham orbitals of all $[\text{Py}-(\text{FA})_2]^-$ complexes. For the complexes structure, the lower part is the Py molecule and the upper part is the FA molecule.

To further understand the impact of different functional groups on the electronic structure of the catalyst-substrate complex, we analyzed the spatial distributions of frontier Kohn-Sham orbitals of all $[\text{Py}-(\text{FA})_2]^-$ (Figure 3). The singly occupied Kohn-Sham orbitals (SOMO) of all anions is distributed at the Py moiety, while the lowest unoccupied Kohn-Sham orbital (LUMO) can be located on different parts of the complex that depends on which specific functional group is added. For the pristine Py, Py-OH, and Py-NH₂, the LUMO is distributed over the FA moiety. For other Py(X), the LUMO is distributed over the Py moiety, and only higher virtual Kohn-Sham orbitals have been found in the FA part, e.g., LUMO+1 for Py-CH=CH₂, Py-C≡C-CH₃, and Py-C≡C-C(CH₃)₃; LUMO+3 for Py-CN and Py-CHO; and LUMO+4 for Py-NO₂ (Figure S2). Given these spatial distributions of frontier Kohn-Sham orbitals, it is more difficult for an electron in the SOMO of a Py(EWGs) to jump to FA than it is for an electron in the SOMO of a Py(EDGs). Therefore, we can conclude from this analysis that the ET process from $\text{Py}(\text{X})^-$ to FA will be energetically more favorable for Py-EDGs than for Py-EWGs.

As mentioned, to simulate the ET process from $\text{Py}(\text{X})$ to FA, the initial and final states are assigned as $[\text{Py}(\text{X})]^--(\text{FA})_2$ and $\text{Py}(\text{X})-[\text{FA}]^-[\text{FA}]$, respectively. The computed Gibbs free energy change between the minimum of each state, ΔG^0 , have been collected in Table 1. This dataset clearly shows that the variation of ΔG^0 goes in two opposite directions: taking pristine Py as the reference point ($\Delta G^0 = 0.03$ eV), EDGs shift ΔG^0 to negative values, while EWGs shift ΔG^0 to more positive values, with strong EWGs (-NO₂, -CN) being more positive than weak EWGs (alkynyl and alkenyl groups). We note that *Lu et al.* reported a ΔG_{ET} (equivalent to ΔG^0) of 0.36 eV for Py-C≡C-C(CH₃)₃ using experimental data and Weller's equation,¹⁴ which is appreciably lower than 0.67 eV by direct calculation using CDFT method. This difference may be due to our simplified model system, which ignores the explicit solvent environment and adopts an incomplete basis set to describe the anion.

We analyzed the ET reaction using a simplified Marcus model. To do so, we noted that a specific C-F bond is longer and deviated more from the FA plane at the final state (Figure S4). This is indicative of the C-F bond activation that may initiate the subsequent HDF reaction. Using the vertical distance change of the activated C-F bond of FA as the one-dimensional reaction coordinate driving the ET, we obtained the potential energy profiles for the initial and final states of $[\text{Py}-(\text{FA})_2]^-$, as shown in Figure 4 and Figure S3. The potential energy profiles of both states are near parabolic, which is a requirement to describe the ET with a Marcus model. Obviously, the ET reactions in all these vdW complexes belong to the normal region,^[21] where the ET rate decreases with the increase of the Gibbs free energy change.

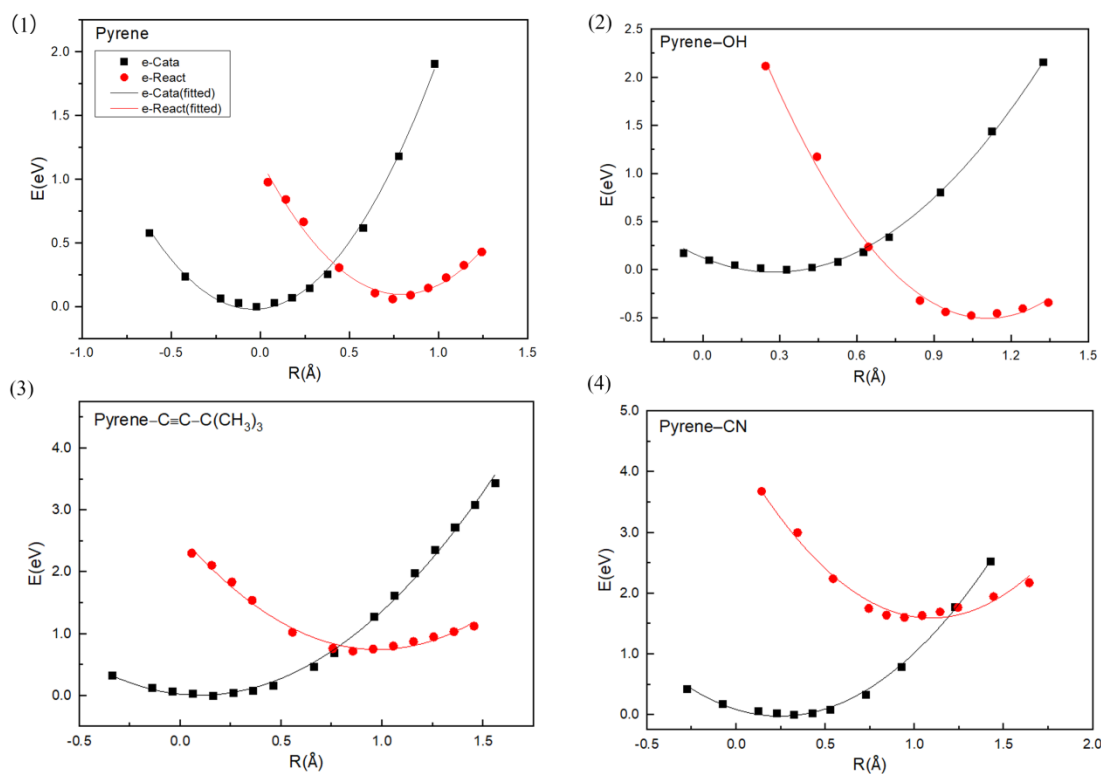


Figure 4: The one-dimensional potential energy profiles of the initial state (black dots) and the final state (red dots) of the catalyst-reactant complex as a function of the reaction coordinate for the ET reaction. E denotes potential energies of the catalyst-reactant complex calculated by CDFT method at $\omega\text{B97XD}/6\text{-}311\text{+G}^{**}$ level. R denotes the reaction coordinate for the ET reaction defined in Figure S4. The initial and final states refer to the states with the excess electron constrained in the catalyst and the reactant, respectively. The solid curves are parabolic fitting of the data included only to guide the eyes.

We then computed the inner-sphere reorganization energies λ associated with each ET reaction using the four-point method,²⁴ Eqn. (1).

$$\lambda = \frac{1}{2} \left\{ \left[E(\text{D}^+ \text{A}^- | \text{DA}) - E(\text{D}^+ \text{A}^- | \text{D}^+ \text{A}^-) \right] + \left[E(\text{DA} | \text{D}^+ \text{A}^-) - E(\text{DA} | \text{DA}) \right] \right\} \quad (1)$$

where $E(\text{X}|\text{Y})$ stands for the potential energy of electronic state X at the optimized geometry of electronic state Y, D refers to the electron donor, and A refers to the electron acceptor. The electron coupling coefficients were computed with the direct coupling method implemented in Q-Chem.²⁵

Based on the calculated ΔG^0 , λ , and V_{if} , we computed the ET rate (k_{ET}) using Eqn. (2).

$$k_{ET} = \frac{2\pi}{h} |V_{if}|^2 \frac{1}{\sqrt{4\pi\lambda k_B T}} \exp\left(\frac{-\Delta G^\ddagger}{k_B T}\right) \quad (2)$$

where h is the reduced Planck constant, k_B is the Boltzmann constant, and T is the temperature. ΔG^\ddagger is the activation energy given as $\Delta G^\ddagger = \frac{1}{4\lambda} (\Delta G^0 + \lambda)^2$.

These results have been collected in Table 1. Note that this simplified formulation of the Marcus model is intended only to provide a qualitative estimate of the ET rates, indicating the general effect of adding an EDG or EWG to the catalyst (See note in the ‘‘Computational Method’’ section). Therefore, the relative ET rates is more important for understanding the impact of added chemical groups than their absolute rate values. Table 1 shows that the ET time (k_{ET}^{-1}) for pristine Py falls in the microsecond regime. The rate is significantly altered as substitution groups are added to Py. While Py-EDGs substantially boost the ET rate, by up to a factor 1000 in $-\text{NH}_2$, Py-EWGs dramatically restrain it. The trend is line with what we found in the electron binding energy of $\text{Py}(\text{X})^-$ anions and their frontier Kohn-Sham orbital distributions as presented above. Importantly, this comparison suggests that chemical group modification can be an effective knob to tune the ET property of organic photocatalysts. Among all quantities contributing to the rate, the free energy change of ET plays a dominant

role in determining the relative value of k_{ET} , indicating that it can be used as a descriptor that facilitates us to study the modulation of a specific type of ET reaction.

Table 1. Comparison of reorganization energies, free energy changes, activation energies, electron coupling coefficients, the absolute and relative ET rates for various of Py(X)-(FA)₂ anionic complexes.

Py(X)-(FA) ₂	λ /eV	ΔG^0 /eV	ΔG^\ddagger /eV	V_{if} /eV	k_{ET} /s ⁻¹	k_{rel}
-H	1.43	0.03	0.38	-0.03	7.28×10^6	1
-OH	1.55	-0.27	0.27	-0.06	1.73×10^9	2.37×10^2
-NH ₂	1.54	-0.58	0.15	-0.03	3.96×10^{10}	5.44×10^3
-CH=CH ₂	1.58	0.53	0.71	0.02	5.13	7.05×10^{-7}
-C≡C-CH ₃	1.51	0.66	0.78	-0.09	8.44	1.16×10^{-6}
-C≡C-C(CH ₃) ₃	1.52	0.67	0.79	0.002	1.90×10^{-3}	2.61×10^{-10}
-CN	1.52	1.50	1.50	0.15	1.61×10^{-11}	2.21×10^{-18}
-CHO	1.51	1.37	1.37	0.05	2.09×10^{-10}	2.87×10^{-17}
-NO ₂	1.67	1.91	1.92	-0.15	1.24×10^{-18}	1.71×10^{-25}

In the framework of the search for metal-free organic photosensitizers and photocatalysts, the lack of physical-chemical knowledge on the ET mechanism has been a handicap in the rational design of new metal-free photocatalysts. For this reason, we have taken photocatalytic hydrodefluorination of polyfluoroarenes (FA) by pyrene-based photocatalysts as a representative model system and conducted a first-principle study on the modulation of ET rates in the framework of Marcus theory. We demonstrate how the chemical modification of Py can affect the ET from Py to FA, a key step in the photochemical process.

The modifications of Py with both electron donating/withdrawing groups can cause a red shift of the maximum absorption wavelength. For Py-(FA)₂ complexes, the light absorption is almost unchanged in regardless of group modifications, suggesting that light harvesting in this system is solely determined by the photocatalyst. All excited Py-(FA)₂ complexes undergo a substantial exothermic relaxation upon receiving an excess electron, which is primarily distributed at the Py moiety. The added EDGs (EWGs) decrease (increase) the electron binding ability of Py⁻ anion, which substantially affects the subsequent ET reaction.

For Py(X)-(FA)₂ anions, the LUMO is distributed over the FA moiety for Py and Py-EDGs (EDGs: -OH and -NH₂), but it stays at the Py moiety for Py-EWGs (EWGs: -CN, -NO₂, -

CHO, etc.), indicating that the ET from Py to FA is energetically more favorable for Py-EDGs than for Py-EWGs. The estimated ET rates show that ET in pristine Py should occur in the microsecond regime. An EDG substitution may increase the ET rate by hundreds or even thousands of times. An EWG substitution, on the other hand, inhibits the ET. We note that ΔG^0 plays a decisive role in determining the trend of ET among different complexes, while the inner-sphere λ is insensitive to chemical modification and V_{if} 's variation with substitution is negligible. We propose that the electron binding energy of catalyst and the free energy change of ET can be used as descriptors for the estimation of relative ET rates for a family of similar species. Finally, we also note that the qualitative differences in the ET rates between the two classes of chromophores is so striking that it implies that adoption of more involved computational models than the bare Py-FA₂ used in our simulations should not significantly change the finds reported here.

In short, our findings provide a comprehensive understanding on the tuning of ET rates for Py-(FA)₂ complexes using chemical group modifications. The information derived from our work can set heuristic rules to be applied to other classes of metal-free organic systems. By exploring more organic chromophores using the same strategy, we are on the way of rational design of new organic photocatalysts.

Computational Method

Density functional theory (DFT) and linear-response time-dependent density functional theory (TDDFT), as implemented the Gaussian 09 program²⁶, were used to study the ground and excited states of Py, FA, and their complexes. To study the ET from Py to FA, the CDFT method was employed using Q-Chem 5.0 program²⁵, to model the approximate diabatic states in which the excess electron is explicitly constrained in either Py or FA. All geometry optimizations and single-point energy calculations employed the range-separated and dispersion-corrected ω B97XD functional²⁷ with the 6-31G(d)²⁸ (for optimization) and 6-311+G(d,p)²⁹ (for single points) basis sets. Normal mode analysis was also carried out at the

same level of geometry optimization to obtain Gibbs free energy for all converged structures. The electronic coupling was calculated with the direct coupling method.³⁰ The solvent effect of diethylacetamide, which was used as the solvent in Lu et al.'s experimental work, was implicitly included by using the corresponding polarizable continuum model (PCM).³¹ For the use of simplified formulation of the semiclassical Marcus model, we keep in mind that it intends only to provide a big picture of the impact of adding an EDG or EWG to the catalyst on the ET rates. This approach will serve as the starting point of future work of accurate calculation of quantitative ET rates involved in organic photocatalytic systems. In addition to the uncertainties in the free energy changes already mentioned, our estimates also do not account for entropic and enthalpic effects in the reorganization energies and completely neglects the outer-sphere variations. The model is also only valid for parabolic potentials sharing comparable harmonic frequency in both states (Table S5), and with this frequency being smaller than the thermal energy. Albeit these latter conditions are all approximately satisfied (see discussion of Table S5), we think the relative ET rates is more important for understanding the impact of added chemical groups than their absolute rate values. For systems with larger frequencies, the rates can be estimated with the help of the Bixon-Jortner model.³²

Supporting Information

The Supporting Information is available free of charge on the ACS Publication website at DOI: 10.1021/xxxx.

Chemical structure of the Py-(FA)₂ complexes (Figure S1); light absorption properties of all Pyrene derivatives (Table S1) and all complex composed of Pyrene derivatives and FA molecule (Table S2); the computed binding energy of each Py-(FA)₂ complex (Table S3); the energy change for the excited complex receiving an excess electron (Table S4); the spatial distribution of higher virtual molecular orbitals of [Py-(FA)₂]⁻ complexes (Figure S2); the one-dimensional potential energy profiles of the initial and final state of the catalyst-reactant complex as a function of the reaction coordinate for the ET reaction (Figure S3); the reaction coordinate for the ET reaction, *R* (Figure S4); the harmonic frequency of the normal mode of the initial state and final state associated to the ET coordinate depicted in Figure 4 (Table S5); The Becke populations of the final state of ET of each [Py(X)-FA₂]⁻ complex given by CDFT calculations (Table S6); and

Cartesian coordinates of all optimized Py-(FA)₂ complexes.

AUTHOR INFORMATION

Corresponding Author

*(G.Z.) E-mail: guozhen@ustc.edu.cn.

*(M.B.) E-mail: mario.barbatti@univ-amu.fr.

ORCID

Guozhen Zhang: 0000-0003-0125-9666

Mario Barbatti: 0000-0001-9336-6607

Note

The authors declare no competing financial support.

Acknowledgments

This work was financially supported by MOST (No. 2016YFA0400904), NSFC (21703221, 21633006), and the Fundamental Research Funds for the Central Universities (WK2060030027). RL and GZ are grateful for the computing resources from the Supercomputing Center of University of Science and Technology of China. MB thanks the support of the Excellence Initiative of Aix-Marseille University (A*MIDEX) and the project Equip@Meso (ANR-10-EQPX-29-01), both funded by the French Government “Investissements d’Avenir” program. MB also acknowledges funding from the WSPLIT project (ANR-17-CE05-0005-01).

References

1. Arceo, E.; Jurberg, I. D.; Alvarez-Fernandez, A.; Melchiorre, P. Photochemical Activity of a Key Donor-Acceptor Complex Can Drive Stereoselective Catalytic Alpha-Alkylation of Aldehydes. *Nat. Chem.* **2013**, *5*, 750-756.
2. Schultz, D. M.; Yoon, T. P. Solar Synthesis: Prospects in Visible Light Photocatalysis. *Science* **2014**, *343*, 1239176.

3. Jin, J.; MacMillan, D. W. Alcohols as Alkylating Agents in Heteroarene C-H Functionalization. *Nature* **2015**, *525*, 87-90.
4. Romero, N. A.; Nicewicz, D. A. Organic Photoredox Catalysis. *Chem. Rev.* **2016**, *116*, 10075-10166.
5. Liu, Q.; Wu, L.-Z. Recent Advances in Visible-Light-Driven Organic Reactions. *Natl. Sci. Rev.* **2017**, *4*, 359-380.
6. Ravelli, D.; Dondi, D.; Fagnoni, M.; Albini, A. Photocatalysis. A Multi-Faceted Concept for Green Chemistry. *Chem. Soc. Rev.* **2009**, *38*, 1999-2011.
7. Arias-Rotondo, D. M.; McCusker, J. K. The Photophysics of Photoredox Catalysis: A Roadmap for Catalyst Design. *Chem. Soc. Rev.* **2016**, *45*, 5803-5820.
8. Ravelli, D.; Protti, S.; Fagnoni, M. Carbon-Carbon Bond Forming Reactions Via Photogenerated Intermediates. *Chem. Rev.* **2016**, *116*, 9850-9913.
9. Ischay, M. A.; Anzovino, M. E.; Du, J.; Yoon, T. P. Efficient Visible Light Photocatalysis of [2+2] Enone Cycloadditions. *J. Am. Chem. Soc.* **2008**, *130*, 12886-12887.
10. Du, J.; Espelt, L. R.; Guzei, I. A.; Yoon, T. P. Photocatalytic Reductive Cyclizations of Enones: Divergent Reactivity of Photogenerated Radical and Radical Anion Intermediates. *Chem. Sci.* **2011**, *2*, 2115-2119.
11. Neumann, M.; Zeitler, K. A Cooperative Hydrogen-Bond-Promoted Organophotoredox Catalysis Strategy for Highly Diastereoselective, Reductive Enone Cyclization. *Chem. Eur. J.* **2013**, *19*, 6950-6955.
12. Lima, C. G. S.; de M. Lima, T.; Duarte, M.; Jurberg, I. D.; Paixão, M. W. Organic Synthesis Enabled by Light-Irradiation of Eda Complexes: Theoretical Background and Synthetic Applications. *ACS Catal.* **2016**, *6*, 1389-1407.
13. Silvi, M.; Arceo, E.; Jurberg, I. D.; Cassani, C.; Melchiorre, P. Enantioselective Organocatalytic Alkylation of Aldehydes and Enals Driven by the Direct Photoexcitation of Enamines. *J. Am. Chem. Soc.* **2015**, *137*, 6120-6123.
14. Lu, J.; Khetrupal, N. S.; Johnson, J. A.; Zeng, X. C.; Zhang, J. "Pi-Hole-Pi" Interaction Promoted Photocatalytic Hydrodefluorination Via Inner-Sphere Electron Transfer. *J. Am. Chem. Soc.* **2016**, *138*, 15805-15808.
15. Pirnot, M. T.; Rankic, D. A.; Martin, D. B.; MacMillan, D. W. Photoredox Activation for the Direct Beta-Arylation of Ketones and Aldehydes. *Science* **2013**, *339*, 1593-1596.
16. Lang, X.; Chen, X.; Zhao, J. Heterogeneous Visible Light Photocatalysis for Selective Organic Transformations. *Chem. Soc. Rev.* **2014**, *43*, 473-486.
17. Twilton, J.; Le, C.; Zhang, P.; Shaw, M. H.; Evans, R. W.; MacMillan, D. W. C. The Merger of Transition Metal and Photocatalysis. *Nat. Rev. Chem.* **2017**, *1*, 0052.
18. Theriot, J. C.; Lim, C. H.; Yang, H.; Ryan, M. D.; Musgrave, C. B.; Miyake, G. M. Organocatalyzed Atom Transfer Radical Polymerization Driven by Visible Light. *Science* **2016**, *352*, 1082-1086.
19. Pearson, R. M.; Lim, C. H.; McCarthy, B. G.; Musgrave, C. B.; Miyake, G. M. Organocatalyzed Atom Transfer Radical Polymerization Using N-Aryl Phenoxazines as Photoredox Catalysts. *J. Am. Chem. Soc.* **2016**, *138*, 11399-11407.
20. McCarthy, B. G.; Pearson, R. M.; Lim, C. H.; Sartor, S. M.; Damrauer, N. H.; Miyake, G. M. Structure-Property Relationships for Tailoring Phenoxazines as Reducing Photoredox Catalysts. *J. Am. Chem. Soc.* **2018**, *140*, 5088-5101.

21. Kumpulainen, T.; Lang, B.; Rosspeintner, A.; Vauthey, E. Ultrafast Elementary Photochemical Processes of Organic Molecules in Liquid Solution. *Chem. Rev.* **2017**, *117*, 10826-10939.
22. Marcus, R. A. Electron Transfer Reactions in Chemistry: Theory and Experiment (Nobel Lecture). *Angew. Chem. Int. Ed.* **1993**, *32*, 1111-1121.
23. Kaduk, B.; Kowalczyk, T.; Van Voorhis, T. Constrained Density Functional Theory. *Chem. Rev.* **2012**, *112*, 321-370.
24. Wu, Q.; Van Voorhis, T. Direct Calculation of Electron Transfer Parameters through Constrained Density Functional Theory. *J. Phys. Chem. A* **2006**, *110*, 9212-9218.
25. Shao, Y.; Gan, Z.; Epifanovsky, E.; Gilbert, A. T. B.; Wormit, M.; Kussmann, J.; Lange, A. W.; Behn, A.; Deng, J.; Feng, X.; et al. Advances in Molecular Quantum Chemistry Contained in the Q-Chem 4 Program Package. *Mol. Phys.* **2014**, *113*, 184-215.
26. Frisch, M. J.; Trucks, G. W.; Schlegel, H. B.; Scuseria, G. E.; Robb, M. A.; Cheeseman, J. R.; Scalmani, G.; Barone, V.; Mennucci, B.; Petersson, G. A.; et al. *Gaussian 09*, Revision D.01; Gaussian, Inc.: Wallingford, CT, USA, 2013.
27. Chai, J. D.; Head-Gordon, M. Long-Range Corrected Hybrid Density Functionals with Damped Atom-Atom Dispersion Corrections. *Phys. Chem. Chem. Phys.* **2008**, *10*, 6615-6620.
28. Francl, M. M.; Pietro, W. J.; Hehre, W. J.; Binkley, J. S.; Gordon, M. S.; DeFrees, D. J.; Pople, J. A. Self-Consistent Molecular Orbital Methods. Xxiii. A Polarization-Type Basis Set for Second-Row Elements. *J. Chem. Phys.* **1982**, *77*, 3654-3665.
29. Clark, T.; Chandrasekhar, J.; Spitznagel, G. W.; Schleyer, P. V. R. Efficient Diffuse Function-Augmented Basis Sets for Anion Calculations. Iii. The 3-21+G Basis Set for First-Row Elements, Li-F. *J. Comput. Chem.* **1983**, *4*, 294-301.
30. Farazdel, A.; Dupuis, M.; Clementi, E.; Aviram, A. Electric-Field Induced Intramolecular Electron Transfer in Spiro π -Electron Systems and Their Suitability as Molecular Electronic Devices. A Theoretical Study. *J. Am. Chem. Soc.* **1990**, *112*, 4206-4214.
31. Tomasi, J.; Mennucci, B.; Cammi, R. Quantum Mechanical Continuum Solvation Models. *Chem. Rev.* **2005**, *105*, 2999-3093.
32. Brédas, J.-L.; Beljonne, D.; Coropceanu, V.; Cornil, J. Charge-Transfer and Energy-Transfer Processes in π -Conjugated Oligomers and Polymers: A Molecular Picture. *Chem. Rev.* **2004**, *104*, 4971-5004.